Elsevier has created a Monkeypox Information Center in response to the declared public health emergency of international concern, with free information in English on the monkeypox virus. The Monkeypox Information Center is hosted on Elsevier Connect, the company's public news and information website.

Elsevier hereby grants permission to make all its monkeypox related research that is available on the Monkeypox Information Center - including this research content - immediately available in publicly funded repositories, with rights for unrestricted research re-use and analyses in any form or by any means with acknowledgement of the original source. These permissions are granted for free by Elsevier for as long as the Monkeypox Information Center remains active.

Virology 449 (2014) 120–132

Contents lists available at ScienceDirect

Virology

journal homepage: www.elsevier.com/locate/yviro

Susceptibility of the wild-derived inbred CAST/Ei mouse to infection by orthopoxviruses analyzed by live bioluminescence imaging

Jeffrey L. Americo, Cindy L. Sood, Catherine A. Cotter, Jodi L. Vogel, Thomas M. Kristie, Bernard Moss *, Patricia L. Earl **

Laboratory of Viral Diseases, National Institute of Allergy and Infectious Diseases, National Institutes of Health, Bethesda, MD 20892, USA

ARTICLE INFO

Article history:
Received 26 September 2013
Returned to author for revisions
28 October 2013
Accepted 7 November 2013
Available online 28 November 2013

Keywords:
Poxvirus pathogenesis
Vaccinia virus pathogenesis
Cowpox virus pathogenesis
Wild-derived inbred mice

ABSTRACT

Classical inbred mice are extensively used for virus research. However, we recently found that some wild-derived inbred mouse strains are more susceptible than classical strains to monkeypox virus. Experiments described here indicated that the 50% lethal dose of vaccinia virus (VACV) and cowpox virus (CPXV) were two logs lower in wild-derived inbred CAST/Ei mice than classical inbred BALB/c mice, whereas there was little difference in the susceptibility of the mouse strains to herpes simplex virus. Live bioluminescence imaging was used to follow spread of pathogenic and attenuated VACV strains and CPXV virus from nasal passages to organs in the chest and abdomen of CAST/Ei mice. Luminescence increased first in the head and then simultaneously in the chest and abdomen in a dose-dependent manner. The spreading kinetics was more rapid with VACV than CPXV although the peak photon flux was similar. These data suggest advantages of CAST/Ei mice for orthopoxvirus studies.

Published by Elsevier Inc.

Introduction

The mouse is widely used for infectious disease research because of its many advantages including the availability of highly inbred strains (Beck et al., 2000). Inbred mice can be divided into classical and wild-derived groups. Commonly used laboratory mice belong to the classical group, which are genetically similar to each other and are derived from a small number of progenitors (Goios et al., 2007; Ideraabdullah et al., 2004). In contrast, wild-derived strains are genetically diverse, having been trapped at different locations and times prior to inbreeding. We recently screened a large number of inbred strains of mice for susceptibility to monkeypox virus (MPXV) infection (Americo et al., 2010). Of these, 32 were classical inbred strains and 6 were wild-derived. Remarkably, all the classical inbred strains were highly resistant to intranasal MPXV infection, whereas three of the wild-derived strains were susceptible. The most susceptible was CAST/Ei (abbreviated CAST), derived from a wild population of the subspecies Mus musculus castaneous trapped in a grain warehouse in Thailand. The vulnerability of CAST mice to MPXV correlated with a low interferon-γ response following intranasal infection (Earl et al., 2012). However, CAST mice are not immunodeficient, as vaccination provided complete protection against MPXV (Americo et al., 2010). In addition, the CAST mouse has been reported to be resistant to infection with flaviviruses (Sangster et al., 1993). We are unaware of CAST mouse studies with other infectious agents, although resistance to influenza virus is predicted based on the presence of the interferon regulated Mx gene (Staeheli et al., 1988) and this mouse strain is susceptible to Bacillus anthracus lethal toxin (Moayeri et al., 2004).

We were interested in determining whether the susceptibility of CAST mice to MPXV would extend to other members of the orthopoxvirus genus of the chordopoxvirus subfamily of the Poxviridae (Damon, 2013; Moss, 2013). Vaccinia virus (VACV) and cowpox virus (CPXV) were chosen for this investigation as they are extensively used for pathogenesis, vaccine and anti-viral drug studies in mice (Bray et al., 2000; Smee et al., 2000, 2001). Here we report that that the LD_{50} values for VACV and CPXV are two logs lower in CAST mice than in BALB/c mice, providing an advantage as a model system. However, there was no significant difference in the susceptibility of CAST and BALB/c mice to herpes simplex virus 1 (HSV-1), an unrelated double-stranded DNA virus. Virus titration and bioluminescence imaging were used to track the spread of phenotypically different strains of VACV and CPXV in the CAST mouse.

Results

Susceptibility of CAST and BALB/c mice to VACV

We previously reported that CAST mice are highly sensitive to intranasal infection with MPXV and that the LD_{50} is 680 PFU

* Correspondence to: 33, North Drive, Bethesda, MD 20814, USA. Tel.: +1 301 496 9869; fax: +1 301 480 1147.
** Correspondence to: 33, North Drive, Bethesda, MD 20814, USA. Tel.: +1 301 402 4112.
E-mail addresses: bmoss@nih.gov (B. Moss), pearl@nih.gov (P.L. Earl).

0042-6822/$ - see front matter Published by Elsevier Inc.
http://dx.doi.org/10.1016/j.virol.2013.11.017

(Americo et al., 2010). In contrast, BALB/c mice exhibited little disease and no mortality when infected with doses of MPXV as high as 10^7 PFU. To determine whether the vulnerability of CAST mice to MPXV extended to other orthopoxviruses, we infected CAST and BALB/c mice intranasally with escalating doses of VACV strain Western Reserve (WR). Previous studies had indicated that the LD_{50} for VACV WR in BALB/c mice was between 10^4 and 10^5 PFU. In compliance with NIH guidelines, animals that lost 30% of their weight or appeared moribund were terminated; therefore reported deaths included both natural occurrences and euthanasia. In the experiment depicted in Fig. 1, BALB/c mice were infected intranasally with 10^2 through 10^6 PFU. Weight loss was rapid and severe at the two highest doses of 10^5 and 10^6 PFU (Fig. 1B) with death of all animals by day 9 after infection (Fig. 1D). Weight loss was delayed and less severe with each successive reduction in infectious dose. With the 10^4 PFU challenge, only one animal out of 10 succumbed and there was no mortality in the 10^3 and 10^2 PFU groups. This experiment was repeated with similar results and the LD_{50} for the combined data was 2.2×10^4 PFU.

CAST mice were infected intranasally with 10^{-1} through 10^4 PFU of VACV WR. Mice that received the three lowest doses (0.1, 1 and 10 PFU) showed no weight loss or signs of disease (Fig. 1A). The 0.1 and 1 PFU doses were inadequate to produce a systemic infection as determined by the absence of antibody production or protection against a subsequent lethal challenge dose (Fig. S1). However, the 10 PFU group produced specific antibody and was protected against challenge (Fig. S1). Weight loss and signs of disease started at a dose of 10^2 PFU (Fig. 1A). At the latter dose, 50% of the animals died between days 6 and 13 (Fig. 1C). Animals that received 10^3 or 10^4 PFU died more rapidly. The LD_{50} of VACV WR for CAST mice was 1×10^2 PFU, more than two logs lower than the same virus in BALB/c mice and more than a half log lower than MPXV in CAST mice.

Previous studies have shown that VACV WR disseminates to lungs, spleen and brain following intranasal infection (Law et al., 2005). To determine the extent of virus spread and replication of VACV WR in CAST mice, organs were removed from each mouse that died from the infection. The organs were frozen and subsequently thawed and homogenized. VACV titers were determined by plaque assay and expressed as yield per gram of tissue. Extensive spread to lung, liver, spleen, brain, and kidney was found in all animals with higher yields from animals infected with 10^3 and 10^4 PFU than from those infected with 10^2 PFU (Fig. 1G). Because the ovaries were too small to accurately weigh, we expressed the yield as total PFU (Fig. 1H). Extensive replication was found in the ovaries of all CAST mice irrespective of input dose, consistent with the known predilection of VACV WR for this organ (Karupiah et al., 1990).

ACAM2000, a licensed vaccine for smallpox, is highly attenuated in comparison to VACV WR. We infected CAST and BALB/c mice with doses of ACAM2000 ranging from 10^4 to 10^7 PFU to see if disease symptoms occurred in either mouse model. CAST mice in all dosage groups became hunched and scruffy, developed antibodies and were protected against weight loss following challenge with a lethal dose of VACV WR (Fig. S2). CAST mice that received 10^7 PFU of ACAM2000 lost weight transiently but recovered fully by day 10 post-infection (Fig. 1E). No weight loss occurred in BALB/c mice regardless of the dose; only the 10^7 PFU group became scruffy and even they fully recovered. Thus, although infection of either mouse strain with ACAM2000 did not produce any deaths, there was greater morbidity in the CAST mice.

Susceptibility of CAST and BALB/c mice to CPXV-Brighton (CPXV-Br)

Next, we compared the susceptibility of the two mouse strains to intranasal infection with CPXV-Br. BALB/c mice infected with 10^4 PFU exhibited weight loss during the second week, but all recovered by day 22 (Fig. 2B). Weight loss was accelerated in the 10^5 and 10^6 PFU groups and nearly all died between days 8 and 12 (Fig. 2D). The LD_{50} for CPXV-Br in BALB/c mice was estimated to be 3.6×10^4 PFU. CAST mice were infected with 10^1–10^6 PFU. All CAST mice, even at the low dose of 10^1 PFU, became hunched and those infected with 10^2 PFU or more lost some weight (Fig. 2A). Weight loss was accelerated and more severe at the higher doses. The time to death and number of mice that died were inversely and directly related to the virus dose, respectively (Fig. 2C). At the lower doses, deaths occurred over a period of several weeks. The extent of weight loss did not correlate well with death at inoculation doses lower than 10^4 PFU. The LD_{50} for CPXV-Br in CAST mice was 10^2 PFU, two logs lower than in BALB/c mice. CAST mice survived longer after infection with lethal doses of CPXV-Br (Fig. 2C) than with VACV WR (Fig. 1C) and the differences were significant at doses of 10^3 ($p=0.0005$) and 10^4 ($p=0.001$).

Virus spread was assessed in CAST mice by removal of organs in all animals that died. Organs were harvested on the day of death and stored frozen in buffer. After thawing and homogenization, CPXV-Br titers were determined by plaque assay. As shown in Fig. 2E, there was extensive replication in all organs examined: lung, liver, spleen and brain. Overall, the CPXV-Br organ titers were slightly lower than the VACV-WR titers and there were some differences in the relative amounts in the different organs such as the brain.

Intranasal infection of CAST mice with poxviruses expressing firefly luciferase (LUC)

In the previous section, we measured the amounts of virus in various organs at the time of death. In order to follow spread in individual animals during the course of infection, we employed recombinant viruses that express firefly LUC, which were previously used for cell entry studies. WRvFire (Townsley et al., 2006), IHD-JvFire (Bengali et al., 2009), and Wyeth-vFire (Bengali et al., 2009) were derived from the VACV WR, VACV IHD-J and Wyeth vaccine (DryVax) strains, respectively. CPXV-Br-luc (Bengali et al., 2012) was derived from CPXV-Br. In each case, the LUC open reading frame was regulated by the same synthetic early/late promoter (Chakrabarti et al., 1997) and inserted between the F12L and F13L open reading frames (Copenhagen VACV nomenclature). To ascertain whether the gene insertion and expression of LUC diminished virulence, we infected CAST mice intranasally with 10^1, 10^2, or 10^3 PFU of WRvFire, IHD-JvFire, or CPXV-Br-luc, respectively, and followed weight loss and death for up to 24 days. The patterns for weight loss and mortality of WRvFire (Fig. 3A and D) closely mimicked that of the parental VACV WR (Fig. 1A and C), and were similar to that of IHD-JvFire (Fig. 3B and E). Weight loss and mortality appeared more severe with CPXV-Br-luc (Fig. 3C and F) than with the parental CPXV-Br (Fig. 2A and C). However, this was likely due to the difference in age of animals in the two experiments. CAST mice infected with CPXV-Br (Fig. 2A and C) were 14–15 weeks old and those infected with CPXV-Br-luc (Fig. 3C and F) were 8 weeks old. Survival analysis indicated significant differences between WRvFire and CPXV-Br-luc ($p=0.006$) and IHD-JvFire and CPXV-Br-luc ($p=0.009$) but not between the two VACV strains ($p=0.389$) at the dose of 10^3 PFU.

Bioluminescence imaging of CAST mice infected with WRvFire

Groups of CAST mice were infected intranasally with 10, 100 or 1000 PFU of WRvFire and repeatedly imaged over a period of 3 weeks. D-Luciferin was injected into the peritoneum and the LUC signal was captured with an IVIS 200 imager. All the animals in the 100 and 1000 PFU groups exhibited bioluminescence, whereas only two of the four inoculated with 10 PFU were infected. Images

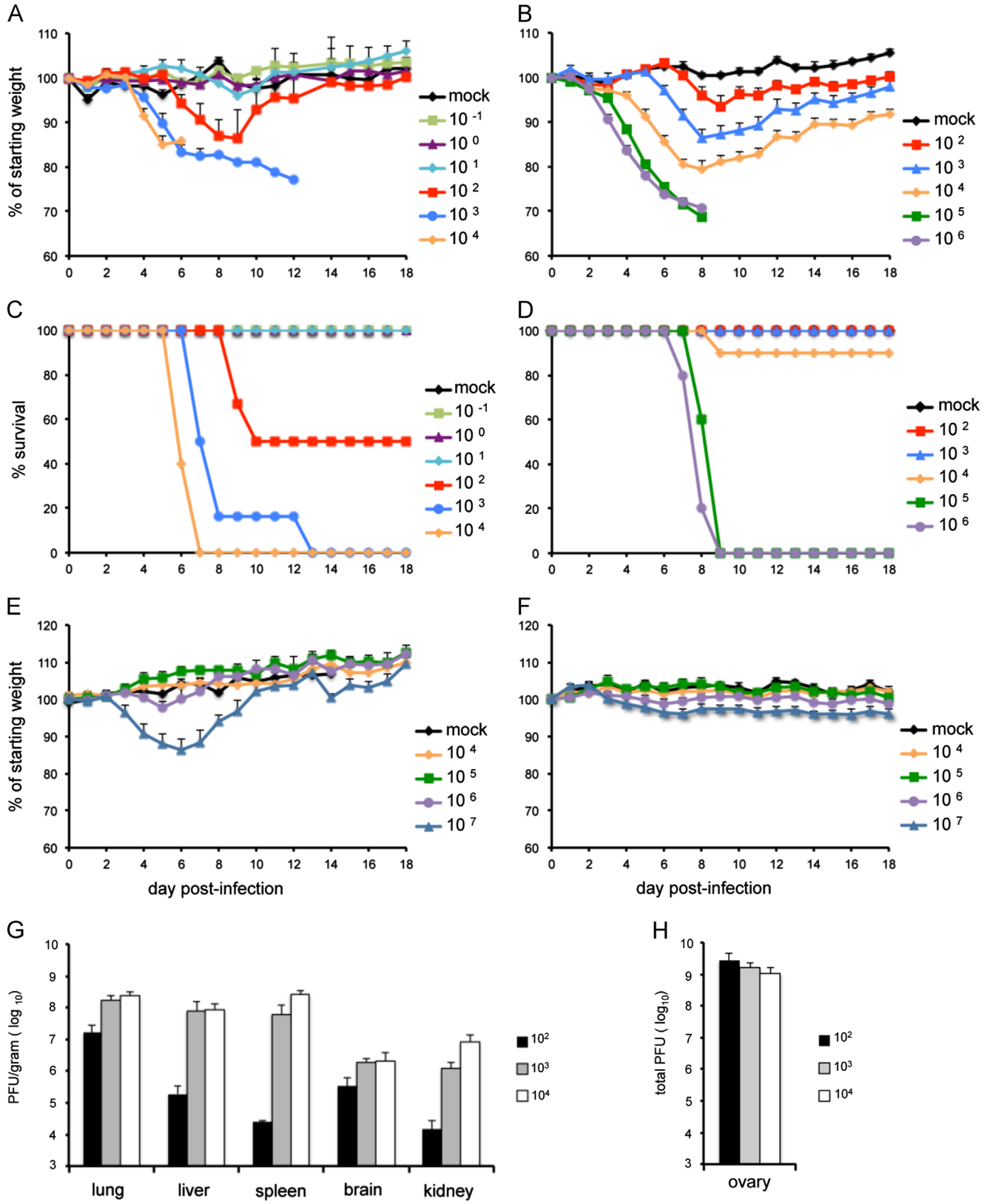

Fig. 1. Weight loss and survival of CAST and BALB/c mice following intranasal infection with VACV WR or ACAM2000. Groups of 4–10, 14–15 weeks old female CAST and 11 weeks old BALB/c mice were infected intranasally with escalating doses of VACV WR or ACAM2000. Animals were monitored daily for weight loss and death for 18 days. Weight loss (A) and survival (C) of CAST mice infected with VACV WR; weight loss (B) and survival (D) of BALB/c mice infected with VACV WR; weight loss of CAST mice (E) and BALB/c mice (F) infected with ACAM2000; virus titers on the day of death in lung, liver, kidney, spleen and brain (G) and ovaries (H) of CAST mice infected with VACV WR. Bars represent standard error of the mean (SEM).

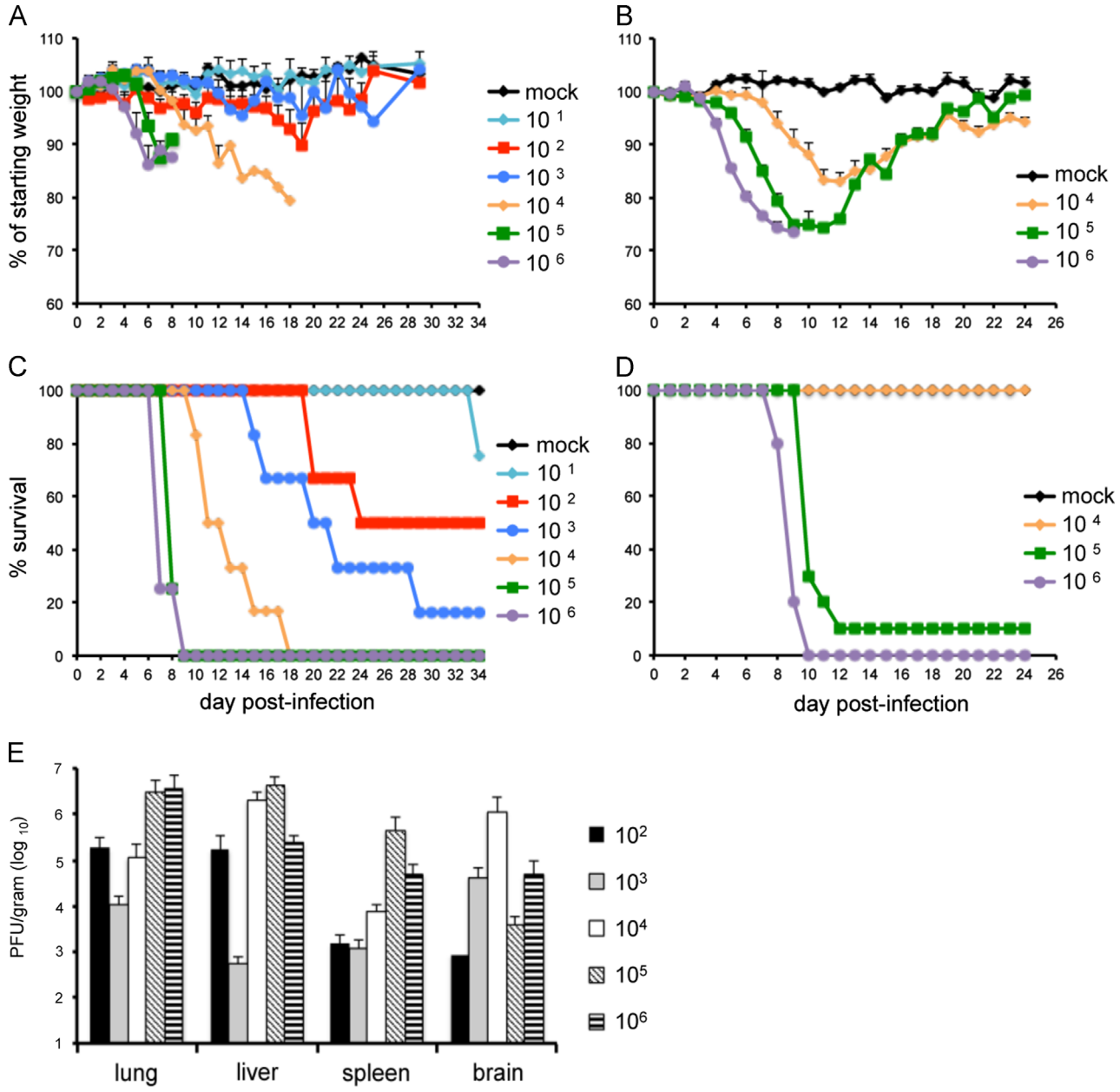

Fig. 2. Weight loss and survival of CAST and BALB/c mice following intranasal infection with CPXV-Br. Groups of 3–10, 14–15 weeks old female CAST and 11 weeks old BALB/c mice were infected intranasally with escalating doses of CPXV-Br. Animals were monitored daily for weight loss and death for up to 34 days. Weight loss (A) and survival (C) of CAST mice; weight loss (B) and survival (D) of BALB/c mice; (E) virus titers on the day of death in organs of CAST mice. Bars represent SEM.

from representative animals infected with 10 PFU (Fig. 4A), 100 PFU (Fig. 4B) and 1000 PFU (Fig. 4C) are presented. Because luminescence was far greater in the head than the body, we showed a 1 s exposure for the head and 10 s exposure for the torso. Regions of interest (ROI) were drawn for the head, chest, and abdomen. The photon flux was calculated using Living Image software and the values for animals in each group were averaged. Luminescence was first detected in the head and then simultaneously in the chest and abdomen (Fig. 4D–F). The maximum total photon flux in the head was greater than 10^9 photon/s/cm^2 and peaked on day 7–8 in all groups. This likely includes virus replication in the nasal passage, the site of primary infection. The maximum total photon flux was greater than one log lower in the torso than the head. The peak for the abdomen (days 4–7) preceded the peak for the chest (days 7–9). Luminescence from the ROIs drawn on the chest and abdomen was primarily from the lungs and from the liver and spleen, respectively (data not shown). Since the rib cage reduces the amount of light emission from the lungs relative to that from the liver and spleen, the total photon flux from the chest and abdomen cannot be directly compared. However, comparisons can be made between animals infected with different doses of virus within each designated area. There was a clear dose–response in the rate and total amount of replication in the head, chest, and abdomen (Fig. 4D–F), which correlated with weight loss and mortality (Fig. 3A and D). All animals infected with 1000 PFU died by day 9 post-infection, two of the four infected with 100 PFU died by day 8 while the other two recovered. The virus titers in the organs of dead animals indicated extensive replication (Fig. S3A), as found in the previous experiment (Fig. 1G and H).

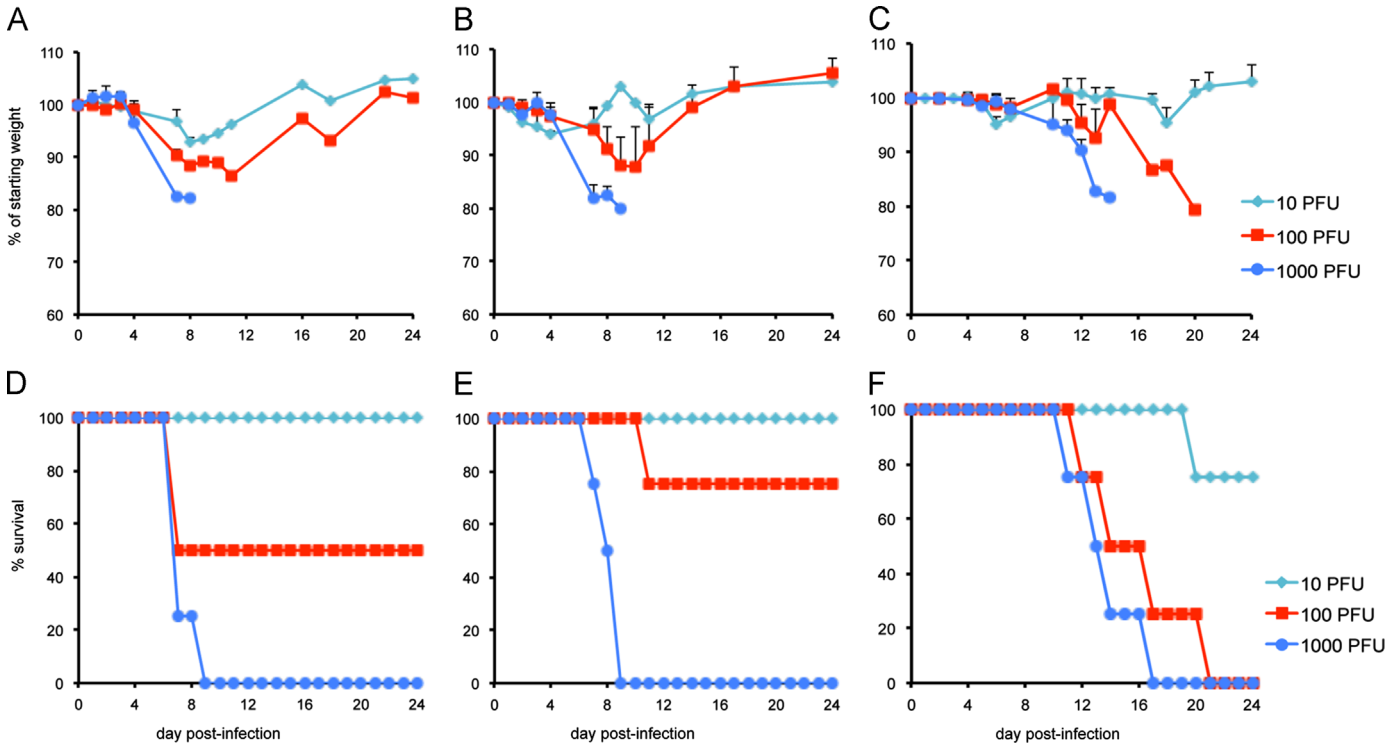

Fig. 3. Intranasal infection of CAST mice with LUC-expressing viruses. Groups of four 8–10 week old female mice were infected intranasally with 10, 100, or 1000 PFU of WRvFire, IHD-JvFire, or CPXV-Br-luc. Animals were monitored daily for 24 days for weight loss and death. Weight loss of mice infected with WRvFire (A), IHD-JvFire (B) and CPXV-Br-luc (C); survival of mice infected with WRvFire (D), IHD-JvFire (E), and CPXV-Br-luc (F). Bars represent SEM.

Bioluminescence imaging of BALB/c mice infected with WRvFire

To compare the pattern of virus spread and replication in CAST mice with that in less susceptible BALB/c mice, we infected groups of BALB/c mice intranasally with 5×10^3, 5×10^4, or 5×10^5 PFU of WRvFire. Animals were weighed and imaged for 18 days unless they succumbed earlier to the infection. Animals in all groups lost weight but this was more rapid and pronounced at the two higher input doses. The number of imaging days of animals infected with 5×10^5 and 5×10^4 was reduced because they all died by days 9 and 10, respectively. Only one animal in the 5×10^3 group died and this was on day 12. Images from representative animals in each group are shown in Fig. 5A (5×10^3 PFU), Fig. 5B (5×10^4 PFU), and Fig. 5C (5×10^5 PFU). As occurred with CAST mice, luminescence was much higher in the head than in the body, requiring longer exposure times and head covering in order to accurately capture images in the body. Kinetics of replication as quantitated by total photon flux in the head (Fig. 5D), chest (Fig. 5E), and abdomen (Fig. 5F) was averaged for all animals within each group and was similar to that found with CAST mice (Fig. 4D–F), allowing for the difference in the inoculum doses. Notably, the input required for similar levels of replication was more than 2 logs higher in BALB/c than in CAST mice. As with CAST mice, high titers of virus were recovered from organs of all animals that died (data not shown).

Bioluminescence imaging of CAST mice infected with IHD-JvFire

The IHD-J and WR strains of VACV exhibit differences in mode of spread and cell entry in cell culture (Bengali et al., 2009; Blasco et al., 1993; Mercer et al., 2010; Payne, 1980), making it interesting to compare them in mouse models. In a previous comparison of BALB/c mice infected intranasally with 10^5 PFU of WRvFire and an IHD-J LUC recombinant, Zaitseva et al. (2011) found higher bioluminescence of the WR recombinant than the IHD-J recombinant in the nasal cavity and lungs but similar levels in the liver and spleen. In the present study, CAST mice were infected intranasally with 10, 100, or 1000 PFU of IHD-JvFire. Images of a representative animal from each infection group are shown in Fig. 6A–C. The total photon flux was averaged for animals in each group and the kinetics of virus spread in three regions of the body was determined (Fig. 6D–F). Luminescence in the head displayed kinetics similar to that found with WRvFire with a peak on days 7–8 and maximum of greater than 10^9 photon/s/cm^2 in the 100 and 1000 PFU groups. Only one animal in the 10 PFU group displayed any luminescence with a maximum photon flux of 3.5×10^8. At the two higher doses, replication was considerably more extensive in both areas of the torso with IHD-JvFire than it was with WRvFire. Specifically, at the input dose of 1000 PFU, the peak photon flux in the chest was 1.5×10^9 with IHD-JvFire, while it was 9.5×10^7 with WRvFire. In the abdomen, the maximum was 9.5×10^9 with IHD-JvFire and 9.4×10^7 with WRvFire. At the input dose of 100 PFU, greater replication was also observed with IHD-JvFire than with WRvFire, although the contrast was not as striking. At the input dose of 10 PFU, little difference was seen between the two viruses. In addition to measuring luminescence, organs of those animals that died were titered confirming higher levels of IHD-JvFire than WRvFire except in the brain and turbinates (Fig. S3B).

Bioluminescence imaging of CAST mice infected with Wyeth-vFire

Next, we imaged CAST mice infected with Wyeth-vFire, which was derived from the same attenuated DryVax vaccine strain as ACAM2000. Due to the attenuation, we only infected animals at the high dose of 10^7 PFU. Images of a representative animal are

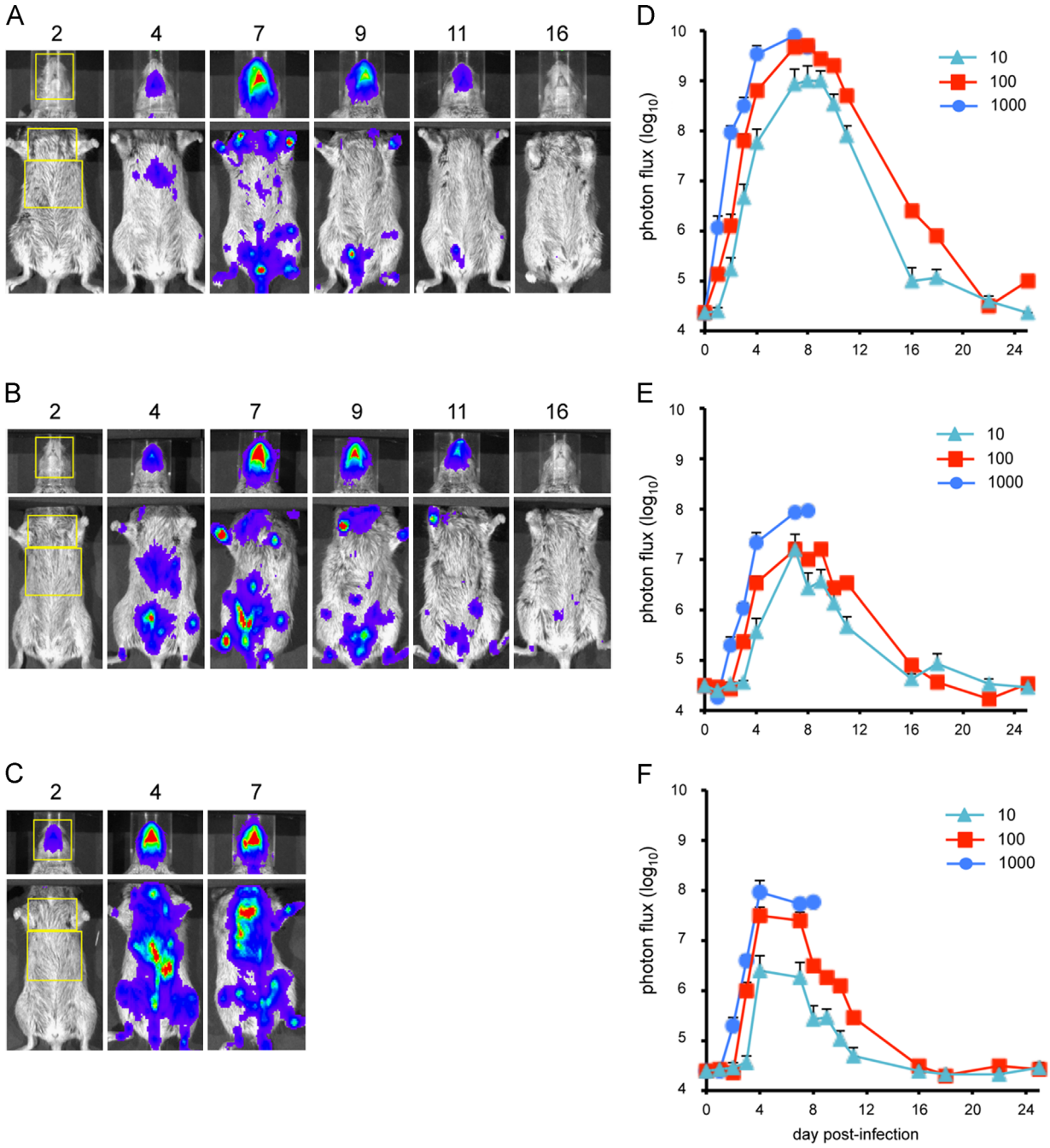

Fig. 4. Bioluminescence imaging of CAST mice infected with WRvFire. Three groups of four female CAST mice were infected intranasally with (A) 10 PFU, (B) 100 PFU, or (C) 1000 PFU of WRvFire. Representative images of the heads and ventral torsos of infected mice are shown. The number above each image is the day post-infection. The yellow boxes outline the regions of interest (ROI) used to calculate photon flux. Relative LUC expression is represented by a pseudocolor heat map in which red indicates a high number of photon counts and blue indicates a low number of photon counts. Bioluminescent images of the head were obtained using an f/stop of 1, binning factor of 4, and an acquisition time of 1 s, while images of the ventral torso were obtained with an f/stop of 1, binning factor of 8, and an acquisition time of 10 s. The same color scale set between 600 and 60,000 was used for all three panels of pictures. To quantify bioluminescence signals as total photon flux (photon/s/cm^2/sr), ROI analysis was performed on the (D) head, (E) chest, and (F) abdomen of infected mice. Data represent mean group values for photon flux. Bars represent SEM.

shown in Fig. 7A and quantitation of luminescence of three animals is in Fig. 7B. Strong bioluminescence was detected in the head, which reached a maximum of greater than 10^9 photon/s/cm^2, a value similar to that found in animals infected with 1000 PFU of the more virulent WR and IHD-J strains. Spread to the lungs peaked on day 5 with a maximum of 1.5×10^6 photon/s/cm^2. However, there was very little spread to the abdomen and virus was completely cleared from all animals by day 15.

Bioluminescence imaging of CAST mice infected with CPXV-Br-luc

Groups of CAST mice were infected intranasally with 10, 100, or 1000 PFU of CPXV-Br-luc and imaged repeatedly over a period of 3 weeks. Images of a representative animal from each group are shown in Fig. 8A–C and the average luminescence values in the head, chest and abdomen in Fig. 8D, E, and F, respectively. The peak luminescence and the speed of infection were proportional to the dose. As with VACV, luminescence increased most rapidly in

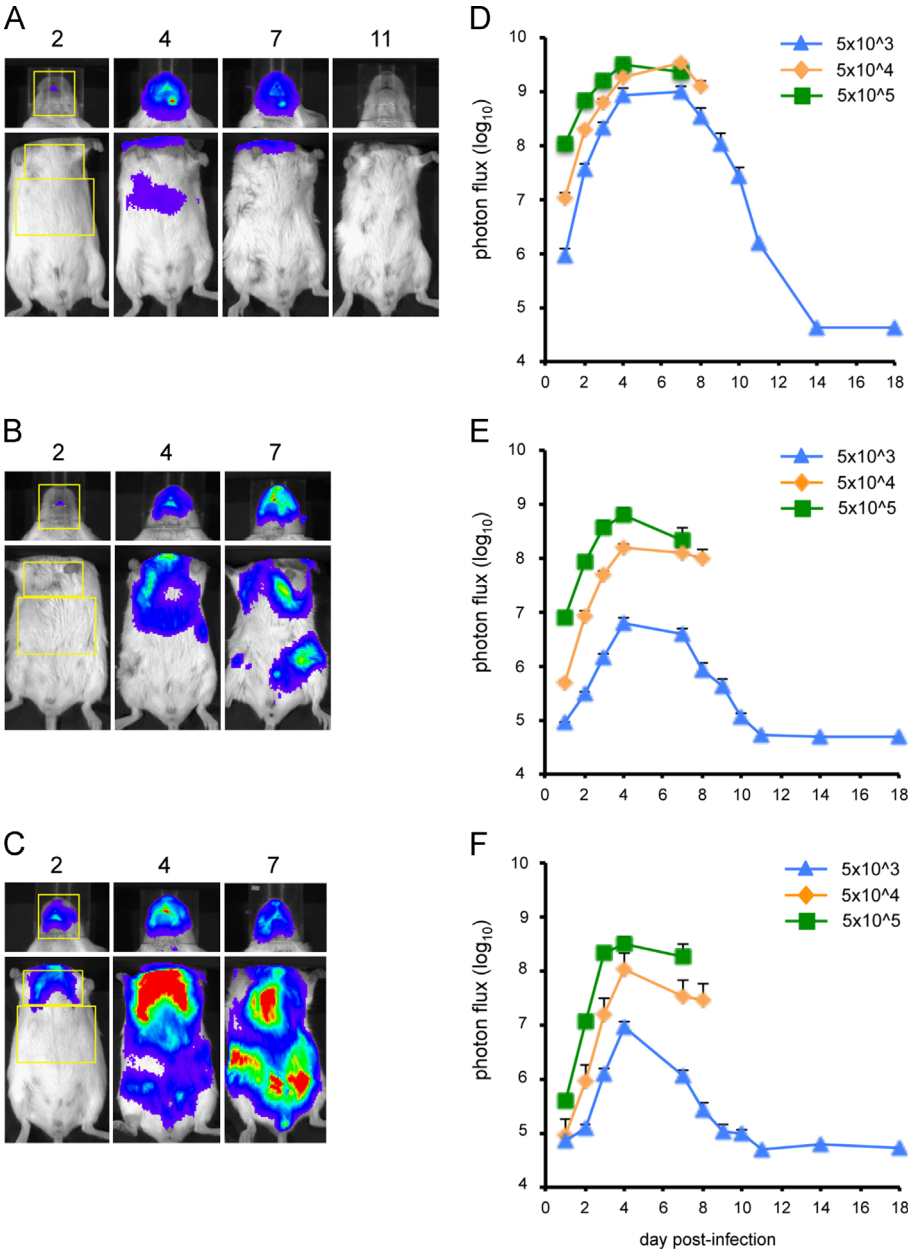

Fig. 5. Bioluminescence imaging of BALB/c mice infected with WRvFire. Three groups of five female BALB/c mice were infected intranasally with (A) 5×10^3 PFU, (B) 5×10^4 PFU, or (C) 5×10^5 PFU of WRvFire. Representative images of the heads and ventral torsos of infected mice are shown with the day post-infection indicated above the images. The yellow boxes outline the ROI used to calculate photon flux. Bioluminescence images of the head were obtained using an f/stop of 1, binning factor of 4, and an acquisition time of 1 s, while images of the ventral torso were obtained with an f/stop of 1, binning factor of 8, and an acquisition time of 10 s. In panel A the color scale was 600–30,000; for panels B and C it was 4000–60,000. Quantification of bioluminescence signals, expressed as photon flux (photons/s/cm^2/sr), is shown for the head (D), chest (E), and abdomen (F). Data represent mean group values for photon flux. Bars represent SEM.

the head, followed by the chest and abdomen. However, the kinetics of spread was slower with CPXV-Br-luc than with WRvFire and IHD-JvFire. The peak flux in the heads of the two VACV strains occurred on days 7–8, while luminescence with CPXV-Br-luc was still increasing on days 9–10 when the mice infected with 1000 and 100 PFU died; the peak occurred on day 16 in the mice infected with 10 PFU. The course of CPXV spread in the chest and abdomen was also much slower than with VACV.

Direct comparison of virus spread in CAST mice infected with 100 PFU of WRvFire, IHD-JvFire, or CPXV-Br-luc

To directly compare spread of WRvFire, IHD-JvFire and CPXV-Br-luc, we infected CAST mice with 100 PFU of each virus in the same experiment. Mice infected with WRvFire or IHD-JvFire rapidly lost weight with maximum loss between days 8 and 12 (data not shown). Three of the four mice infected with WRvFire and two of the four mice infected with IHD-JvFire died between days 7 and 10. Weight loss in CPXV-Br-luc-infected mice was not observed until day 13 and three of the four mice died between days 17 and 19, a week later than that seen in the WRvFire and IHDJ-vFire-infected groups (data not shown). This delayed disease of CPXV compared to VACV was reflected in the spread and replication of virus shown in the quantitation of luminescence signals (Fig. 9). Kinetics of WRvFire and IHD-JvFire replication was similar to each other in the head, chest and abdomen. Although the luminescence values in the chest and abdomen were higher with IHD-J compared to WR, this difference did not reach

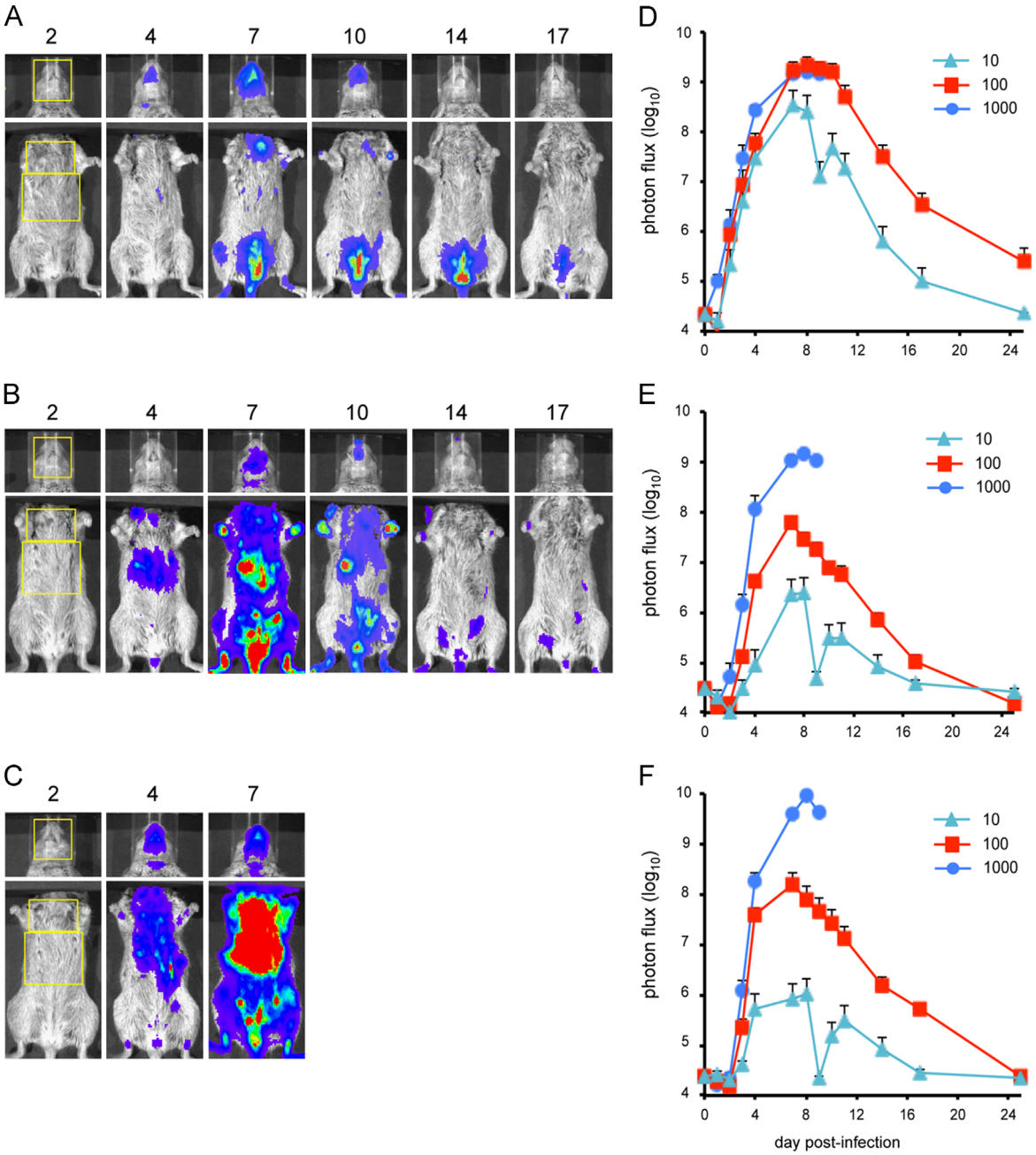

Fig. 6. Bioluminescence imaging of CAST mice infected with IHD-JvFire. Three groups of four female CAST mice were infected intranasally with (A) 10 PFU, (B) 100 PFU, or (C) 1000 PFU of IHDJ-vFire. The day post-infection on which images were obtained are indicated above each image. The yellow boxes outline the ROI used to calculate photon flux. Bioluminescent images of the head were obtained using an f/stop of 1, binning factor of 4, and an acquisition time of 1 s. Images of the ventral torso were acquired using an f/stop of 1, binning factor of 8, and an acquisition time of 10 s. The same color scale set between 600 and 60,000 was used for all three picture panels. ROI analysis was performed on the (D) head, (E) chest, and (F) abdomen of infected mice to calculate total photon flux. Data represent mean group values for photon flux. Bars represent SEM (the low photon flux values on day 9 was probably due to poor injection of substrate).

statistical significance. The peak luminescence values in CPXV-Br-luc were similar to that of WRvFire and IHD-JvFire at all three sites; however, the times to reach the peak in CPXV-Br-luc were delayed by 7–10 days in comparison to the other two viruses.

Infection of CAST and BALB/c mice with HSV-1

We compared the susceptibility of CAST and BALB/c mice to HSV-1 in order to determine if the difference with orthopoxviruses extended to an unrelated large, double stranded DNA virus. Weight loss of CAST and BALB/c mice infected intranasally with 5×10^3–5×10^6 PFU are shown in Fig. 10A and B, respectively. Although BALB/c mice lost more weight than did CAST mice at the higher doses ($p < 0.05$ on days 2–5 and days 6–8 in animals infected with 10^6 and 10^5 PFU, respectively), the percent survival and time-to-death were similar in the two strains (Fig. 10C). LD_{50} values of 3×10^5 and 5×10^5 PFU were calculated for CAST and BALB/c, respectively. Trigeminal ganglia were removed from all surviving animals and viral DNA was quantified by qPCR. Although yields were slightly higher in CAST mice than BALB/c mice (Fig. 10E), the difference was not statistically significant.

Both strains of mice were also infected by the ocular route with 5×10^4–1×10^6 PFU of HSV-1. Survival was similar in the two strains of mice (Fig. 10D) with LD_{50} values of 7.9×10^4 and 5.6×10^5 in CAST and BALB/c mice, respectively. In a subsequent experiment, 15 mice from each strain were infected with a

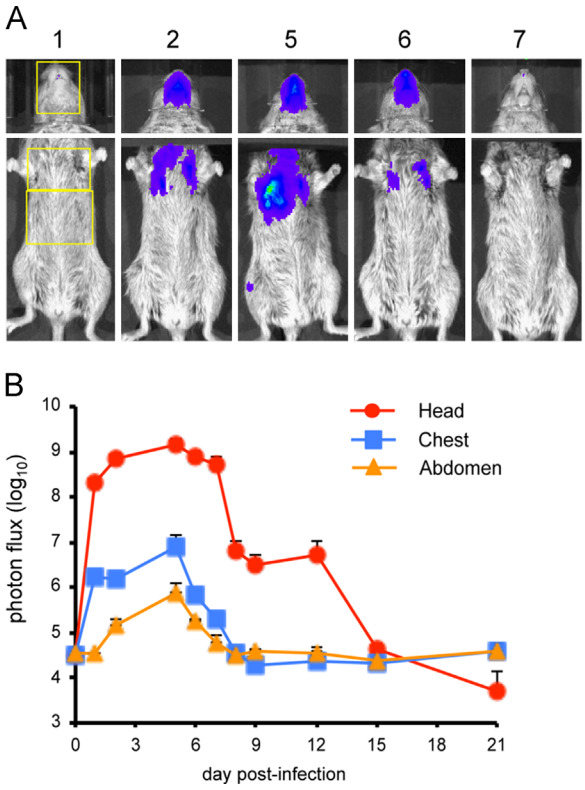

Fig. 7. Bioluminescence imaging of CAST mice infected with Wyeth-vFire. Three female CAST mice were infected intranasally with 10^7 PFU of Wyeth-vFire. (A) Representative images of the heads and ventral torsos. The day post-infection on which images were obtained is indicated above each image. The yellow boxes outline the ROI used to calculate photon flux. Bioluminescent images of the head were obtained using an f/stop of 1, binning factor of 4, and an acquisition time of 1 s. The same color scale set between 600 and 60,000 was used for all three panels of pictures. Images of the ventral torso were acquired using an f/stop of 1, binning factor of 8, and an acquisition time of 60 s. (B) ROI analysis was performed on the head, chest, and abdomen of infected mice to calculate total photon flux. Data represent mean group values for photon flux. Bars represent SEM.

sub-lethal dose of 5×10^4 PFU. On day 6 post-infection, mice were euthanized, trigeminal ganglia removed, and viral DNA quantified. As shown in Fig. 10F, similar amounts of DNA were found in CAST and BALB/c mice.

Discussion

Most virus infection studies have been carried out with classical inbred mouse strains that have limited genetic diversity and are composed of a mosaic of genomes from Mus musculus subspecies. There is greater diversity among wild-derived strains that were captured from various parts of the world and inbred separately. Indeed, in a screen of 38 inbred mouse strains, the 32 classical strains were all resistant to challenge with MPXV whereas deaths occurred in three of the six wild-derived strains (Americo et al., 2010). The most sensitive strain was CAST/EiJ, a subspecies of Mus musculus castaneous that was derived from a small number of founder mice captured in Thailand. We subsequently found that CASA/RkJ, which was independently inbred from the same founder population as CAST/EiJ, was also sensitive to MPXV (our unpublished data). A literature search revealed only one other study of the susceptibility of CAST or CASA to virus infection. The two mouse strains were both resistant to the flaviviruses Murray Valley encephalitis virus and yellow fever virus as measured by lethality and virus replication following intracerebral challenge (Sangster et al., 1993). The flavivirus resistance gene was ultimately mapped to a member of the 2′–5′-oligoadenylate synthetase gene family (Perelygin et al., 2002).

The purpose of the present investigation was to determine whether the sensitivity of the CAST mouse was unique to MPXV or extended to other orthopoxviruses and DNA virus families. The classical inbred BALB/c mouse, which is commonly used for VACV and CPXV studies, served for comparison. Using the intranasal route, we found that the LD_{50} values of VACV WR and CPXV Br were each 2 logs lower in CAST mice than BALB/c mice. Titration of the organs of infected CAST mice indicated that the virus had spread from the upper respiratory tract to lungs, brain and abdominal organs. In contrast, BALB/c and CAST mice had a similar susceptibility to intranasal or intraocular inoculation of HSV-1, an unrelated DNA virus. Based on the data obtained with flaviviruses and herpesviruses, there does not seem to be a general vulnerability of CAST mice to virus infection.

Live bioluminescence imaging provides a useful means of following virus spread and recovery in individual animals (Hutchens and Luker, 2007) and has been used with VACV (Luker et al., 2005; Zaitseva et al., 2009) and CPXV (Goff et al., 2007). Three strains of VACV – WR, IHD-J and a derivative of the DryVax vaccine – were used because of their different properties though all were derived from the New York City Department of Health strain. Although WR and IHD-J are neurovirulent strains that were passaged in mouse brains, the latter spreads more rapidly in tissue culture due to more complete release of progeny from the cell surface (Blasco et al., 1993; Payne, 1980). Nevertheless, the kinetics of WR and IHD-J spread in mice was similar and dose dependent. Following intranasal infection, luminescence was first detected in the head, presumably the nasal passages. Luminescence in the chest and abdomen appeared at the same time suggesting independent spread to different organs. Comparison of the photon flux of each virus indicated that WR and IHD-J replicated to a similar extent in the head but that the latter replicated to higher titers in the chest and abdomen. Using a high virus inoculum, we followed the spread of the vaccine strain of VACV. In this case, there was relatively less spread to the chest and abdomen and the attenuated virus was cleared more rapidly than either WR or IHD-J. The kinetics of spread of CPXV-Br was dose dependent and luminescence appeared first in the head and subsequently in the chest and abdomen. CPXV spread was slower than that of the VACV strains, even though the final photon flux was similar. It would be interesting to extend these studies to variola virus, the agent responsible for smallpox, as a small animal model for this human virus does not presently exist.

The sensitivity of CAST mice to MPXV, VACV and CPXV suggests that they either have a susceptibility gene or lack one or more resistance factors that retard orthopoxvirus replication in classical inbred mouse strains. Preliminary studies suggest the latter as the F1 generation of CAST X C57Bl/6 are resistant to MPXV (our unpublished data). Several studies have highlighted the importance of interferon-γ (Giavedoni et al., 1992; Kohonen-Corish et al., 1990; Liu et al., 2004; Sroller et al., 2001; Verardi et al., 2001) in protection against VACV in murine models. Studies with MPXV suggested that an inadequate interferon-γ response in the lung correlated with susceptibility of CAST mice and that exogenous interferon-γ was protective (Earl et al., 2012).

In conclusion, we have established a CAST mouse model for studies of orthopoxvirus infection and spread that has advantages over the use of classical inbred strains. The lethal dose of VACV and CPXV is 100-fold less for CAST mice than for BALB/c mice and the difference is even greater for MPXV.

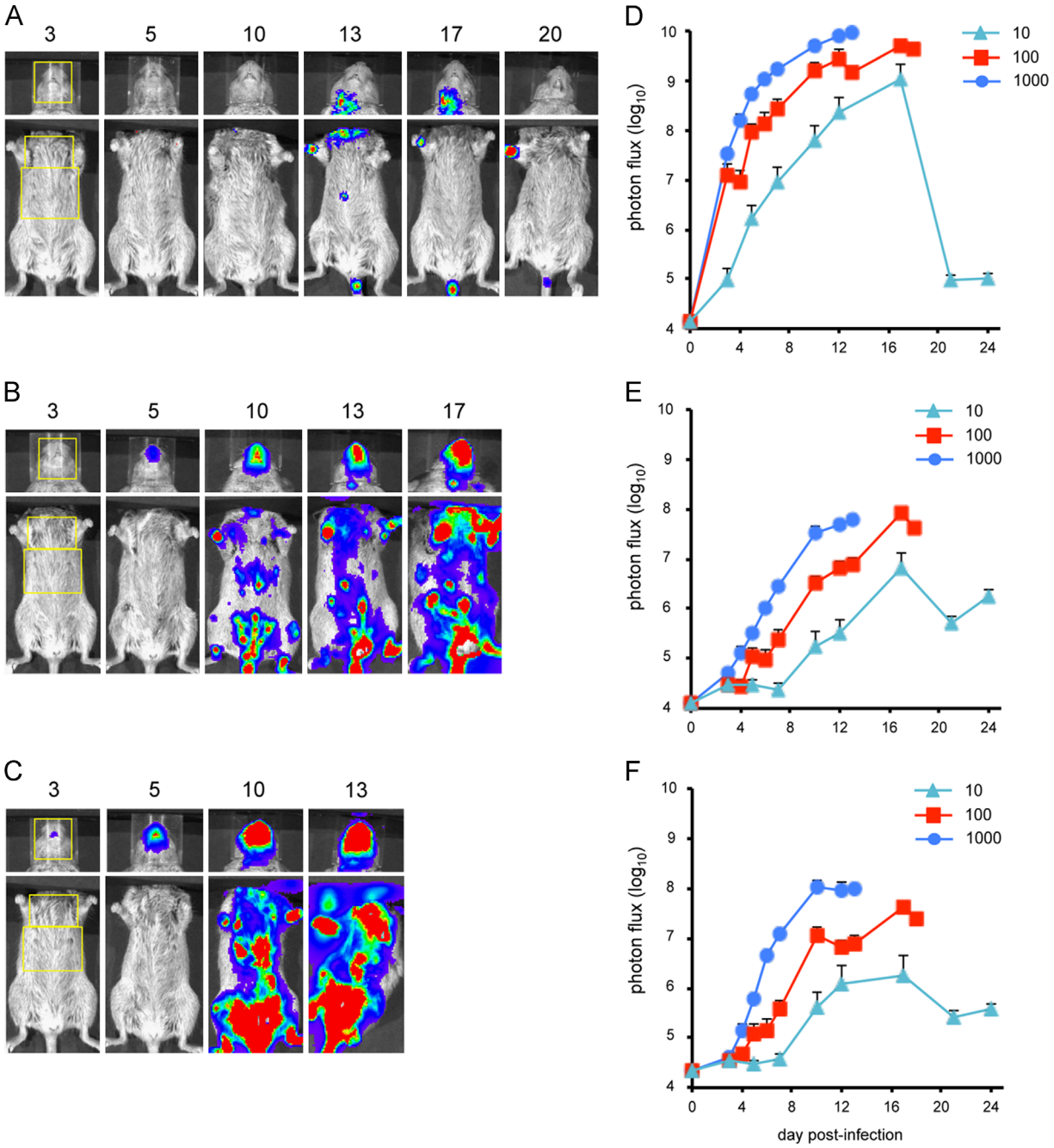

Fig. 8. Bioluminescence imaging of CAST mice infected with CPXV-Br-luc. Three groups of four female CAST mice were infected intranasally with CPXV-Br-luc. Representative images of mice infected with (A) 10 PFU, (B) 100 PFU, or (C) 1000 PFU of CPXV-Br-luc are shown. The day post-infection on which luminescence was measured is indicated above each image. The yellow boxes outline the ROI used to calculate photon flux. Bioluminescent images of the head were obtained using an f/stop of 1, binning factor of 4, and an acquisition time of 1 s. Images of the ventral torso were acquired using an f/stop of 1, binning factor of 8, and an acquisition time of 30 s. Color scales were as follows: 10 PFU inoculum dose, 100–4000 for the head and 100–60,000 for the torso; 100 and 1000 PFU input doses, 2000–60,000. ROI analysis was performed on the (D) head, (E) chest, and (F) abdomen of infected mice to calculate total photon flux. Data represent mean group values for photon flux. Bars represent SEM.

Materials and methods

Cells and viruses

BS-C-1 cells were maintained at 37 °C and 5% CO_2 in modified Eagle minimal essential medium (Quality Biologicals, Inc., Gaithersburg, MD) supplemented with 8% heat-inactivated fetal bovine serum, 10 U of penicillin/ml, 10 μg streptomycin/ml, and 2 mM L-glutamine.

The following strains of VACV were used: WR (ATCC VR-1354) and Wyeth New York City Board of Health from a Wyeth Laboratory DryVax seed stock. CPXV-Br was obtained from ATCC (VR-302). The following recombinant viruses expressing firefly LUC regulated by a synthetic early-late promoter were described previously: WRvFire (Townsley et al., 2006), IHD-JvFire and Wyeth-vFire (Bengali et al., 2009), and CPXV-Br-luc (Bengali et al., 2012). Poxviruses were prepared as previously described (Earl et al., 2001). HSV strain F was prepared and titers were determined according to standard protocols.

Mouse strains

Female CAST/EiJ and BALB/c mice were obtained from Jackson Laboratories (Bar Harbor, ME) and Taconic Biotechnology (Germantown, NY), respectively. Mice were maintained in small, ventilated microisolator cages.

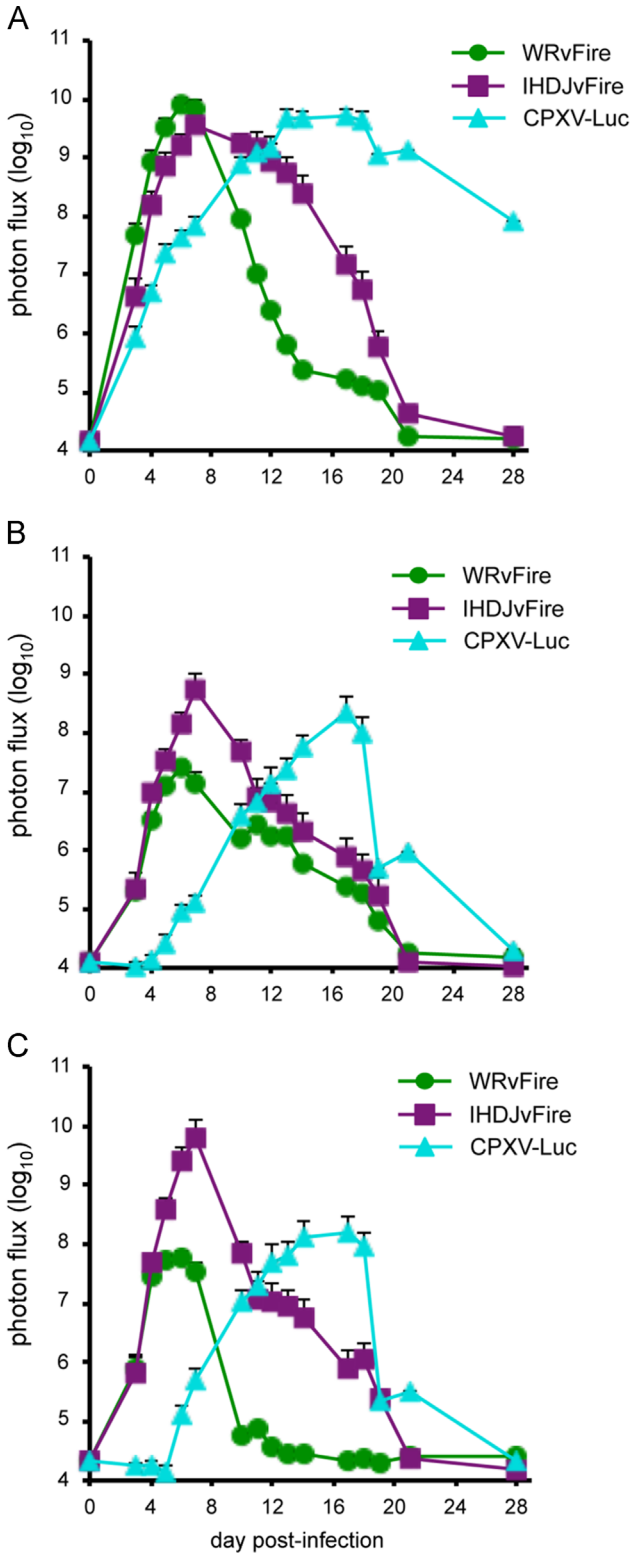

Fig. 9. Kinetics of virus spread in CAST mice infected with WRvFire, IHD-JvFire, or CPXV-Br-luc. Groups of four female CAST mice were infected intranasally with 100 PFU of WRvFire, IHD-JvFire, or CPXV-Br-luc at the same time and imaged for 4 weeks. ROI were drawn on the (A) head, (B) chest, and (C) abdomen of infected mice and total photon flux was calculated. Data represent mean group values for photon flux. Bars represent SEM.

Virus inoculation of animals

On the day of infection, poxviruses were thawed, sonicated and diluted in phosphate buffered saline containing 0.05% bovine serum albumin. The titer of each dose was verified by plaque assay on BS-C-1 cells. For HSV-1, titered, and frozen stocks were used. Intranasal infections were performed by delivery of 10–20 μl of virus into one nostril. For ocular infections, mice were anesthetized with Avertin and virus was deposited on corneas following scarification. Mock-infected animals were inoculated with a similar volume of diluent. In all other experiments, animals were anesthetized by inhalation of isoflurane prior to infection. Animals were weighed and observed five to seven times per week for up to 5 weeks post-infection. Animals that lost 30% of their initial starting weight or became moribund were euthanized in accordance with NIAID Animals Care and Use guidelines. All experiments were performed in an ABSL-2 facility with approval of the NIAID Animal Care and Use Committee.

Statistics

Statistical significance for weight loss, virus titer and luminescence were determined with an unpaired, two-tailed *t* test. Kaplan–Meier survival analysis was performed with GraphPad Prism software.

Bioluminescence imaging

Live imaging was performed with an IVIS 200 system (Perkin Elmer, Waltham, MA). D-Luciferin (Perkin Elmer, Waltham, MA) was injected intraperitoneally (150 μg/g body weight) 10 min prior to imaging. Animals were maintained under isoflurane anesthesia for the duration of the procedure. Animals were imaged daily on weekdays for up to 4 weeks. Luminescent images were collected for 1–60 s with small or medium binning factors. Images of the torso were collected with black paper covering the head to eliminate spill over due to the high luminescence in the head. ROI were drawn around specific anatomic sites and light emission was measured in photons/s/cm^2/sr (photon flux). In the photographs displayed, the color thresholds for each site were constant throughout the time course. Acquisition and analysis were performed with Living Image Software.

Virus titration of infected organs

On the day of death, lung, liver, spleen, brain, kidney, nasal turbinates and ovary were removed, placed in 2–3 ml of balanced salt solution containing 0.1% bovine serum albumin and immediately stored at −80 °C until further use. Organs were thawed and homogenized with a GLH-1 mechanical grinder equipped with a hard-tissue probe (Omni International, Kennesaw, GA). Tissue homogenates were sonicated for three 45 s intervals in tubes immersed in ice water and then centrifuged for 20 s at 400 × *g* in a 4515 microcentrifuge (Eppendorf, Hauppauge, NY). Supernatants were aliquoted and virus titers were determined by plaque assay on BS-C-1 cells.

VACV enzyme-linked immunosorbent assay (ELISA)

Briefly, 96-well plates were coated overnight with 10^6 PFU of purified VACV, fixed with 2% paraformaldehyde for 10 min at 4 °C, and blocked with phosphate-buffered saline containing 5% non-fat dry milk and 0.2% Tween 20 for 1 h at 37 °C. Serum samples were heat inactivated at 56 °C for 30 min. Two-fold serial dilutions were prepared and the plates were incubated at 37 °C for 1 h. After washing, plates were incubated successively with anti-mouse IgG-peroxidase and then BM Blue substrate (Roche Applied Science, Indianapolis, IN). Absorbance was measured at 370 and 492 nm using a Spectramax M5 using Softmax Pro software (Molecular Devices).

qPCR for HSV-1 viral loads

Trigeminal ganglia were harvested from BALB/c and CAST mice post ocular or intranasal infection as described (Liang et al., 2009).

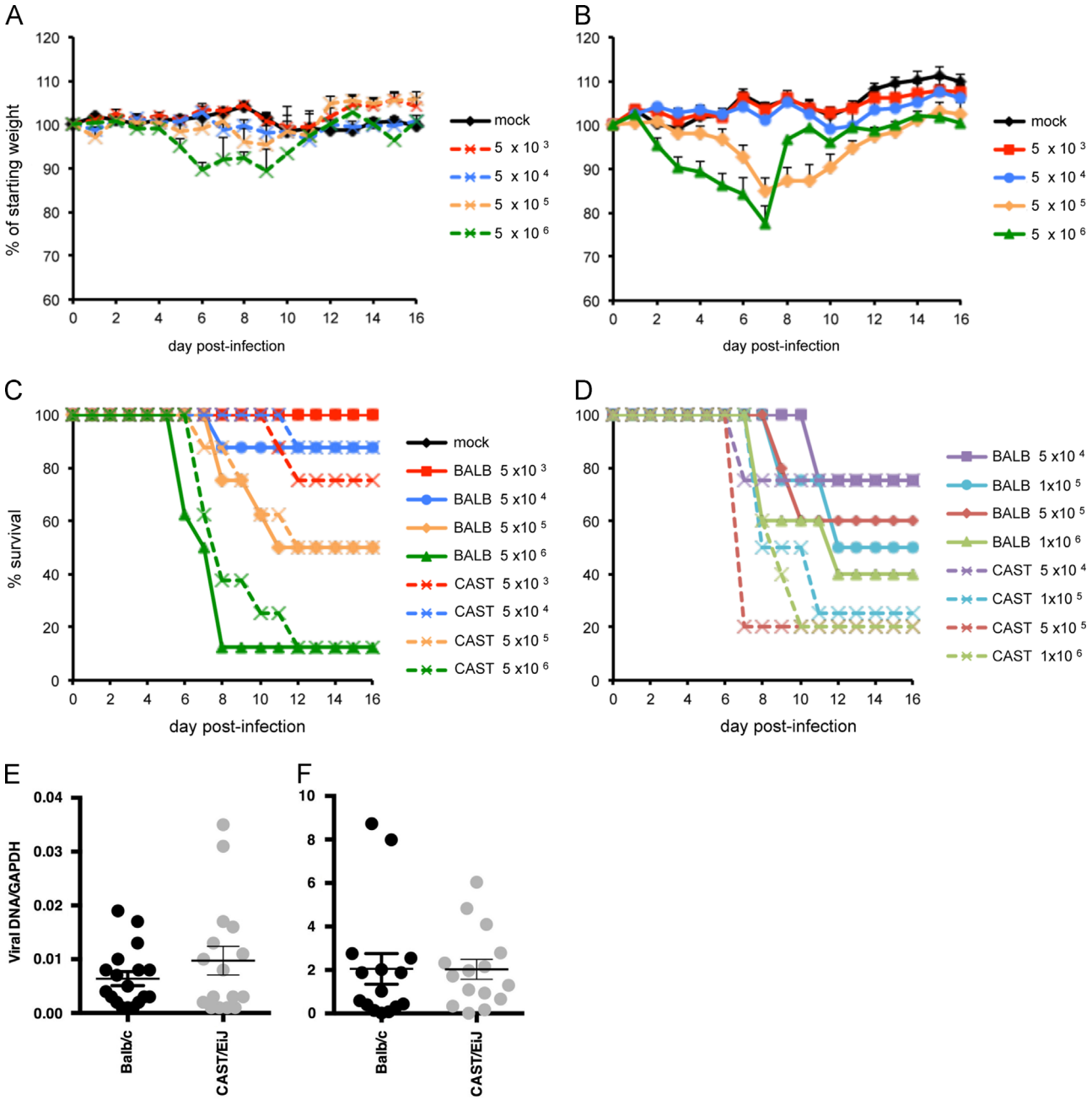

Fig. 10. Infection of CAST and BALB/c mice with HSV-1. CAST (A) and BALB/c (B) mice were infected with 5×10^3–5×10^8 PFU of HSV-1 in one nostril. Daily weights for each group are plotted as the percent of starting weight (mean ± SEM; $n=8$). Survival plots of BALB/c and CAST mice infected with HSV-1 at the indicated infection multiplicities intranasally (C) or via the ocular route (D). Viral DNA loads in trigeminal ganglia of BALB/c and CAST mice infected with HSV-1 (E) intranasally (day 16 post-infection; mean ± SEM; $p=0.1908$; $n=18$) or (F) via the ocular route (day 6 post-infection; mean ± SEM; $p=0.9774$; $n=15$).

Viral DNA was quantified by qPCR using primers to HSV-1 gD (gD-F: GTCAGCGAGGATAACCTGGGG; gD-R: GGGAGGGCGTACTTACAGGAGC) and normalized to the level of cellular glyceraldehyde 3-phosphate dehydrogenase (GAPDH-F: CTGACGTGCCGCCTGGAGAAA; GAPDH-R: CCCGGCATCGAAGGTGGAAGAGT).

Acknowledgments

We thank Gary Luker for helpful discussions on bioluminescence imaging. The research was supported by the Division of Intramural Research, NIAID, NIH.

Appendix A. Supplementary material

Supplementary data associated with this article can be found in the online version at http://dx.doi.org/10.1016/j.virol.2013.11.017.

References

Americo, J.L., Moss, B., Earl, P.L., 2010. Identification of wild-derived inbred mouse strains highly susceptible to monkeypox virus infection for use as small animal models. J. Virol. 84, 8172–8180.
Beck, J.A., Lloyd, S., Hafezparast, M., Lennon-Pierce, M., Eppig, J.T., Festing, M.F., Fisher, E.M., 2000. Genealogies of mouse inbred strains. Nat. Genet. 24, 23–25.
Bengali, Z., Satheshkumar, P.S., Moss, B., 2012. Orthopoxvirus species and strain differences in cell entry. Virology 433, 506–512.

Bengali, Z., Townsley, A.C., Moss, B., 2009. Vaccinia virus strain differences in cell attachment and entry. Virology 389, 132–140.
Blasco, R., Sisler, J.R., Moss, B., 1993. Dissociation of progeny vaccinia virus from the cell membrane is regulated by a viral envelope glycoprotein: effect of a point mutation in the lectin homology domain of the A34R gene. J. Virol. 67, 3319–3325.
Bray, M., Martinez, M., Smee, D.F., Kefauver, D., Thompson, E., Huggins, J.W., 2000. Cidofovir protects mice against lethal aerosol or intranasal cowpox virus challenge. J. Inf. Dis. 181, 10–19.
Chakrabarti, S., Sisler, J.R., Moss, B., 1997. Compact, synthetic, vaccinia virus early/late promoter for protein expression. BioTechniques 23, 1094–1097.
Damon, I., 2013. Poxviruses. sixth ed. In: Knipe, D.M., Howley, P.M. (Eds.), Fields Virology, vol. 2. Wolters Kluwer, Lippincott Williams &Wilkins, Philadelphia, pp. 2160–2184. (2 vols.).
Earl, P.L., Americo, J.L., Moss, B., 2012. Lethal monkeypox virus infection of CAST/EiJ mice is associated with a deficient interferon-gamma response. J. Virol. 86, 9105–9112.
Earl, P.L., Cooper, N., Wyatt, L.S., Moss, B., Carroll, M.W., 2001. Preparation of cell cultures and vaccinia virus stocks. Curr. Protoc. Mol. Biol., 16.16.1–16.16.13.
Giavedoni, L.D., Jones, L., Gardner, M.B., Gibson, H.L., Ng, C.T.L., Barr, P.J., Yilma, T., 1992. Vaccinia virus recombinants expressing chimeric proteins of human immunodeficiency virus and γ-interferon are attenuated for nude mice. Proc. Natl. Acad. Sci. USA 89, 3409–3413.
Goff, A., Twenhafel, N., Garrison, A., Mucker, E., Lawler, J., Paragas, J., 2007. In vivo imaging of cidofovir treatment of cowpox virus infection. Virus Res. 128, 88–98.
Goios, A., Pereira, L., Bogue, M., Macaulay, V., Amorim, A., 2007. mtDNA phylogeny and evolution of laboratory mouse strains. Genome Res. 17, 293–298.
Hutchens, M., Luker, G.D., 2007. Applications of bioluminescence imaging to the study of infectious diseases. Cell. Microbiol. 9, 2315–2322.
Ideraabdullah, F.Y., de la Casa-Esperon, E., Bell, T.A., Detwiler, D.A., Magnuson, T., Sapienza, C., de Villena, F.P., 2004. Genetic and haplotype diversity among wild-derived mouse inbred strains. Genome Res. 14, 1880–1887.
Karupiah, G., Coupar, B., Ramshaw, I., Boyle, D., Blanden, R., Andrew, M., 1990. Vaccinia virus-mediated damage of murine ovaries and protection by virus-expressed interleukin-2. Immunol. Cell Biol. 68, 325–333.
Kohonen-Corish, M.R.J., Long, N.J.C., Woodhams, C.E., Ramshaw, I.A., 1990. Immunodeficient mice recover from infection with vaccinia virus expressing intereferon-γ. Eur. J. Immunol. 20, 157–161.
Law, M., Putz, M.M., Smith, G.L., 2005. An investigation of the therapeutic value of vaccinia-immune IgG in a mouse pneumonia model. J. Gen. Virol. 86, 991–1000.
Liang, Y., Vogel, J.L., Narayanan, A., Peng, H., Kristie, T.M., 2009. Inhibition of the histone demethylase LSD1 blocks alpha-herpesvirus lytic replication and reactivation from latency. Nat. Med. 15, 1312–1317.
Liu, G., Zhai, Q.Z., Schaffner, D.J., Wu, A.G., Yohannes, A., Robinson, T.M., Maland, M., Wells, J., Voss, T.G., Bailey, C., Alibek, K., 2004. Prevention of lethal respiratory vaccinia infections in mice with interferon-alpha and interferon-gamma. Fems Immunol. Med. Microbiol. 40, 201–206.
Luker, K.E., Hutchens, M., Schultz, T., Pekosz, A., Luker, G.D., 2005. Bioluminescence imaging of vaccinia virus: effects of interferon on viral replication and spread. Virology 341, 284–300.
Mercer, J., Knebel, S., Schmidt, F.I., Crouse, J., Burkard, C., Helenius, A., 2010. Vaccinia virus strains use distinct forms of macropinocytosis for host-cell entry. Proc. Natl. Acad. Sci. USA 107, 9346–9351.
Moayeri, M., Martinez, N.W., Wiggins, J., Young, H.A., Leppla, S.H., 2004. Mouse susceptibility to anthrax lethal toxin is influenced by genetic factors in addition to those controlling macrophage sensitivity. Infect. Immun. 72, 4439–4447.
Moss, B., 2013. Poxviridae. sixth ed. In: Knipe, D.M., Howley, P.M. (Eds.), Fields Virology, Vol. 2. Wolters Kluwer, Lippincott Williams &Wilkins, Philadelphia, pp. 2129–2159. (2 vols.).
Payne, L.G., 1980. Significance of extracellular virus in the in vitro and in vivo dissemination of vaccinia virus. J. Gen. Virol. 50, 89–100.
Perelygin, A.A., Scherbik, S.V., Zhulin, I.B., Stockman, B.M., Li, Y., Brinton, M.A., 2002. Positional cloning of the murine flavivirus resistance gene. Proc. Natl. Acad. Sci. USA 99, 9322–9327.
Sangster, M.Y., Heliams, D.B., MacKenzie, J.S., Shellam, G.R., 1993. Genetic studies of flavivirus resistance in inbred strains derived from wild mice: evidence for a new resistance allele at the flavivirus resistance locus (Flv). J. Virol. 67, 340–347.
Smee, D.F., Bailey, K.W., Wong, M.H., Sidwell, R.W., 2000. Intranasal treatment of cowpox virus respiratory infections in mice with cidofovir. Antiviral Res. 47, 171–177.
Smee, D.F., Bailey, K.W., Wong, M.H., Sidwell, R.W., 2001. Effects of cidofovir on the pathogenesis of a lethal vaccinia virus respiratory infection in mice. Antiviral Res. 52, 55–62.
Sroller, V., Ludvikova, V., Maresova, L., Hainz, P., Nemeckova, S., 2001. Effect of IFN-gamma receptor gene deletion on vaccinia virus virulence. Arch. Virol. 146, 239–249.
Staeheli, P., Grob, R., Meier, E., Sutcliffe, J.G., Haller, O., 1988. Influenza virus-susceptible mice carry Mx genes with a large deletion or a nonsense mutation. Mol. Cell Biol. 8, 4518–4523.
Townsley, A.C., Weisberg, A.S., Wagenaar, T.R., Moss, B., 2006. Vaccinia virus entry into cells via a low pH-dependent-endosomal pathway. J. Virol. 80, 8899–8908.
Verardi, P.H., Jones, L.A., Aziz, F.H., Ahmad, S., Yilma, T.D., 2001. Vaccinia virus vectors with an inactivated gamma interferon receptor homolog gene (B8R) are attenuated in vivo without a concomitant reduction in immunogenicity. J. Virol. 75, 11–18.
Zaitseva, M., Kapnick, S.M., Meseda, C.A., Shotwell, E., King, L.R., Manischewitz, J., Scott, J., Kodihalli, S., Merchlinsky, M., Nielsen, H., Lantto, J., Weir, J.P., Golding, H., 2011. Passive immunotherapies protect WRvFire and IHD-J-Luc vaccinia virus-infected mice from lethality by reducing viral loads in the upper respiratory tract and internal organs. J. Virol. 85, 9147–9158.
Zaitseva, M., Kapnick, S.M., Scott, J., King, L.R., Manischewitz, J., Sirota, L., Kodihalli, S., Golding, H., 2009. Application of bioluminescence imaging to the prediction of lethality in vaccinia virus-infected mice. J. Virol. 83, 10437–10447.